

Nanoscale active matter matters: challenges and opportunities for self-propelled nanomotors

Ibon Santiago^{a*}

^a*Department of Physics, University of Oxford, Clarendon Laboratory, Parks Road, Oxford OX1 3PU, United Kingdom*

^{*}*ibon.santiago@physics.ox.ac.uk*

ABSTRACT

Progress in nanotechnology has enabled the synthesis of active particles that can harness chemical energy and translate it into useful work. Catalytic self-propelled motors have implications for understanding out-of-equilibrium systems and have potential applications in active transport at the nanoscale, where they can be used as motors and pumps. Although much research has been done on micron-sized motors, progress in catalytic nanomotors of sub 100 nm is still in its infancy. These nanosized motors are of great importance for future molecular transport at the cellular level because they operate at length scales at which protein motors work. This opinion article focusses on recent advances in the synthesis of catalytic nanomotors and experimental strategies to measure their self-propulsion, which differ from that of micromotors. Enzymatic and metallic nanomotors are surveyed, together with various theoretical models for self-propulsion. Solutions to current challenges are proposed, which include a chemical synthesis approach, new characterisation of motor activity and potential uses of nanomotors in nanomedicine.

Introduction

Molecular motors use chemical energy and transform it into work, orchestrating myriad processes inside a cell. They are examples of active matter, i.e. entities that stay out of thermodynamic equilibrium by consuming energy in the environment (or internally stored) in order to move [1]. There is a growing interest in creating synthetic analogues, not only to reveal and understand new ways of converting energy into motion, but also to use them for transport mechanisms at the nanoscale. Chemically active particles constitute an important

class of active matter systems. Similar to molecular motors, these particles transform chemical energy into motion. These synthetic particles achieve self-propulsion via the catalytic reaction of fuel in their environment and pose interesting theoretical and experimental challenges. Notable examples include Pt/Au nanorods [2], which propel by catalysing a redox reaction, and Janus microswimmers [3], fabricated by coating polystyrene beads with metallic caps, which move by catalysing the reaction only on one hemisphere.

Do these active particles also work at the nanoscale? Insight into this question is essential for cellular level transport. Nanomotors of the length scale at which protein motors work have promising potential in nanomedicine, for example as drug delivery carriers. Apart from applications in areas of nanoscience, active nanomaterials constitute a testbed to better understand the statistical mechanics of non-equilibrium systems [4,5]. Chemically propelled nanomotors could give new insights into locomotion and self-organisation of living organisms and help discover new ways of converting energy into motion yet unseen in nature.

Chemically powered motors have proliferated in the past decade, driven by an interest in achieving smaller autonomous propelled devices [4]. However, progress in synthesising catalytic nanomotors of true nanoscopic scale (<100 nm) is still scarce [6]. The only examples of catalytic nanomotors fall into two categories: metallic and enzymatic nanomotors. Their synthesis, propulsion mechanisms and characterisation methods pose many challenges not found at mesoscopic scales. Solutions to these problems require new approaches and open the door to opportunities in this exciting interdisciplinary area.

Metallic Nanomotors

Both micro and nanomotors face a low Reynolds number regime, where inertial forces are negligible and breaking symmetry is necessary to self-propel [7]. One of the features of metallic catalytic motors is that they break the symmetry by having an asymmetric distribution of metallic catalyst on their surface [4]. This asymmetry translates into the accumulation of reaction products formed on one side of the particle. Usually, two mechanisms are invoked to explain the propulsion by the generation of asymmetric products, namely bubble propulsion [8] and self-diffusiophoresis [9-11]. The former is normally attributed to motors that generate visible bubbles and the latter to those where local bubble generation is negligible and the interaction of products with the surface of the particle leads

to fluid flows that result in the propulsion of the particle [12]. When the catalytic reaction involves a redox process and generates an ionic product, then the propulsion is caused by self-electrophoresis [2,13]. Self-phoretic mechanisms are usually associated with the propulsion of bimetallic nanomotors.

Brownian motion becomes more dominant as motors become smaller. While micromotors lose orientation in a measurable timescale of seconds, nanomotors randomise their direction after μs [14]. This makes a direct measurement of nanomotor velocities experimentally challenging. However, at longer time scales than the reorientation time, self-propulsion is manifested in the form of an increased diffusion coefficient. This means they diffuse with an effective diffusion coefficient D_{eff} that is larger than its equilibrium value D_0 in the absence of a fuel. This is known as *enhanced diffusion* in the literature, and it is the main experimental observable that characterises catalytic nanomotor activity. Multiparticle Collision Dynamic simulations by Kapral and colleagues show that chemically powered motors can operate on very small length scales and yield substantially high velocities and enhanced diffusion, even at Ångström scales [4].

The synthesis of catalytic nanomotors is a major challenge, as achieving asymmetry at the nanoscale is difficult. Shadow-growth physical vapour deposition (PVD) (Figure 1a), a method that worked for micron-sized motors [3], was also adapted to synthesise catalytic nanomotors. Two fabrication mechanisms stand out, which have generated Janus type geometries in sub-100 nm particles. Ma et al. achieved Janus-type geometries using e-beam evaporation of Pt with 60 nm mesoporous silica nanoparticles (Figure 1b) [15]. Even smaller nanomotors have been synthesised by glancing angle deposition (GLAD) of Au onto small Pt nanoparticles to form Au-Pt nanomotors (Figure 1c) [16].

So far, the fabrication of nanomotors has been limited to top-down lithographic methods, and they have involved mostly metallic catalysts [16]. Synthesising even smaller catalytic particles with bespoke shape and distribution of catalyst will require new experimental approaches. One promising way is to use wet-chemical methods. It is a well-established method to obtain asymmetric nanoparticles. The simplicity and effectiveness of wet-chemical synthesis make it a promising tool in active matter research. Recently, self-motile catalytic Janus microparticles were produced by solution phase metallization [17]. Future synthesis

strategies involving established wet-chemical nanotechnology methods would enable fabrication of asymmetric nanoparticles with controllable shape, size and compositions. They could provide a more facile bottom-up approach resulting in a higher throughput of particles. However, these chemical synthesis methods have not yet been exploited in the context of nanomotors. Indeed, further work in this interdisciplinary area is expected.

Enzymatic nanomotors

Catalytic reactions are necessary for chemically-powered self-propulsion. As natural catalysts, enzymes themselves are potential nanomotors. In the past decade, some groups have reported that certain enzymes exhibit enhanced diffusivity in the presence of their substrate [18,19]. Fluorescence Correlation Spectroscopy (FCS) experiments showed that enzymes, including catalase[19,20], urease[18], and alkaline phosphatase[19], undergo enhanced diffusion that depends on substrate concentration. The origin of active motion of these freely diffusing enzymes is still subject to debate. Several theoretical models have been put forward that speculate about the mechanism behind enzymatic self-propulsion, which are listed in Table 1.

The observation of enhanced diffusion for endothermic enzymes [21] as well as exothermic ones [18,19] suggests that the heat generation model proposed by Riedel et al. [19] is not a likely explanation (Figure 2a). On the other hand, stochastic oscillating force dipoles generating hydrodynamic flows that change the diffusion of particles is a stronger hypothesis (Figure 2c). This is supported by experiments with tracer particles [22] and enzymes immobilised on a surface [23] and free in solution [21]. This hypothesis could be verified by single-molecule experiments using FRET, to unravel the conformational changes of enzymes. The investigation of the mechanisms underlying enhanced diffusion in enzymes is still ongoing. Enhanced diffusion of individual enzymes has been challenged by some groups [24], suggesting that this observation could be attributed to a transient quenching of fluorescence caused by catalytic reaction products.

To clarify if enzymes on their own are true nanomotors, other techniques different from FCS that allow the observation of enzyme diffusion in their native state are crucial. Table 3 lists possible experimental methods that can serve this purpose. More experiments addressing this phenomenon will contribute to a complete physical picture of enzymatic propulsion.

Measurement of nanomotor self-propulsion

Most studies on active matter at the micron scale involve the observation of a few natural or synthetic motors in an optical microscope, followed by statistical analysis of their trajectories. The calculation of the mean-squared displacement at short and long time intervals helps distinguish self-propulsion from other sources of motion (e.g. sedimentation, convection, Brownian motion) [25]. However, as particles get smaller, it becomes experimentally more challenging to characterise the dynamics of these motors, and new approaches need to be considered that go beyond fast CCD cameras and improved optics.

As mentioned above, a hallmark of active particles at the nanoscale is the increase in their diffusivity in the presence of their substrate. These could be measured by a number of experimental methods depending on the characteristics of the particles (e.g. size, composition, propulsion mechanism). Dynamic Light Scattering (DLS) is the most commonly used method for particles that scatter light strongly, such as metallic nanomotors. By using this method, Lee and colleagues reported an increase of 25% in diffusion coefficient for 30 nm Au-Pt NP in the presence of 2%(v/v) H_2O_2 (Figure 3 a) [16]. Ma et al. observed a 50% enhancement in diffusion for 40 nm Pt-coated mesoporous silica nanoparticles in higher than 3% (v/v) H_2O_2 (Figure 3 b) [15].

DLS is not commonly used to measure the enhanced diffusion of enzymes, as they do not scatter strongly. Instead, Fluorescence Correlation Spectroscopy (FCS) is a single-molecule method that is used with fluorescently-labelled enzymes (Figure 3c and d). The advantage of this method lies in its selectivity, as only the motion of fluorescent particles is detected, while unlabelled impurities remain undetected. In addition, FCS only requires very low sample concentrations (pM-nM), it can avoid the interference caused by the aggregation of particles and high concentrations of product (e.g. O_2 bubbles). For reliable FCS measurements, it is essential to guarantee that only a single fluorescent species is present in solution. By using this method, catalase[19,20], urease [18], alkaline phosphatase [19], aldolase [21], and DNA polymerase [26] were reported to show enhanced diffusivity at substrate saturation of the order of the bare diffusion coefficient of the enzymes. The enhancement factors in their diffusivity are shown in Table 2.

The field of particle-electrode collisions (also known as nanoimpact voltammetry) provides an alternative to optical or scattering methods, for detecting particles in solution [27,28]. In a

typical nanoimpact experiment, particles collide stochastically on the electrode resulting in characteristic current spikes out of which properties of the particle can be extracted, such as concentration, size and shape. The first work using nanoimpact to track micron size motors was reported recently [29]. This method was also successfully applied for the first time in the context of enzymatic nanomotors [30] (Figure 3 e-f). Nanoimpact experiments allow single-enzyme measurements in their native state, without molecular modifications, using cost-effective experimental setups.

More experimental methods should be introduced to probe nanomotors, ideally in their native state. Nanoparticle tracking analysis (NTA) is a new technique that is capable of tracking particles from about 30 to 1000 nm [31]. NTA and super-resolution setups may also be used to track fluorescent particles by detecting the fluorescence signal rather than the scattered light. While many nanoparticles have been characterised with NTA, their use with nanomotors is still very limited. The advantage and disadvantages of these methods from both theoretical and practical aspects are compared in Table 3. Other promising techniques that can shed light into the dynamics of nanomotors are liquid cell high-resolution electron microscopy [32], diffusion NMR [33] and microscale thermophoresis [34], which have not yet been fully introduced in the context of active matter.

Future applications in active transport

Catalytic nanomotors constitute a rapidly growing field of study that is likely to find applications in active transport at the nanoscale. Given that random thermal energy coexists with active motion, small motors may find applications in systems where rotational diffusion is minimised, such as nano-confined systems [35,36]. We can envision that nanomotors will be used in the near future to transport a nanoscale cargo, especially for drug delivery. The advantage of using nanomotors as drug-delivery systems is that their self-propulsion facilitates tissue penetration and can cross cellular membranes more easily [37]. However, most motors reported so far rely on heavy metals, which are toxic and not suitable for biological use. Therefore, a nanoscale motor system that is biocompatible and biodegradable would be desirable. For this purpose, enzymatic nanomotors are a natural candidate due to their high biocompatibility. One promising direction is to enable the localisation of cargoes on enzymes by using the specificity of DNA hybridisation and using the rich tools of DNA nanotechnology. Crosslinking chemistry (e.g. click-chemistry) allows the conjugation of modified oligonucleotides with functional groups on the surface of the enzyme [38,39]. To

avoid harming the catalytic activity of the native protein, site-specific conjugation of DNA on proteins is possible [40]. These functionalised enzymes could then be bound to various biocompatible cargoes carrying the complementary strand, thus obtaining propulsive cargo/enzymes nanostructures.

The development towards controllable and useful nanomotors is still in its infancy but progressing quickly. New synthesis and detection methods can be envisaged, which will provide high-throughput of nanomotors and improved characterisation of their motion. A better understanding of their propulsion mechanism and the relationship between nanomotors and their environment will facilitate further progress in this promising field. Nanomotors are ideal systems to study nanoscale out-of-equilibrium processes and endowing them with additional properties, like sensing and transport, will make them very attractive for many applications in the future.

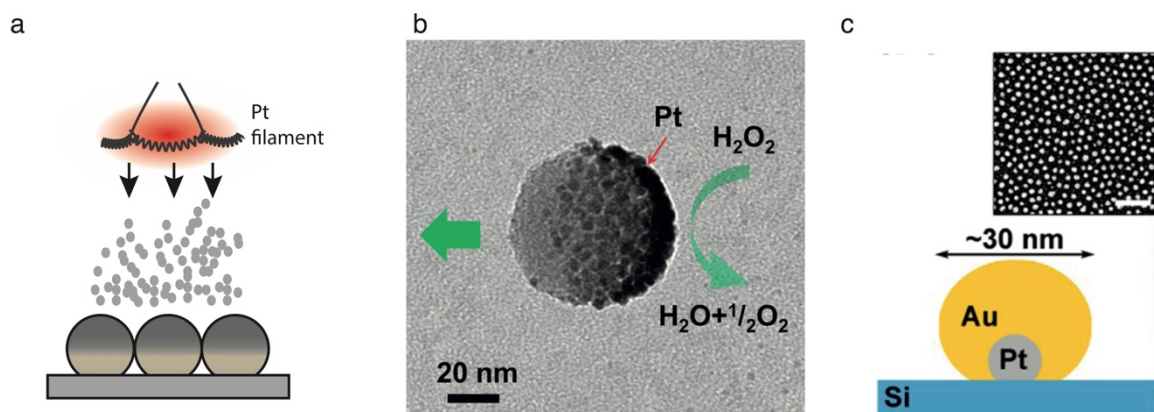


Figure 1 a) Shadow-growth physical vapour deposition (PVD) of metallic catalyst onto microparticles to create half-coated Janus micromotors. b) 65 nm diameter mesoporous silica Janus nanoparticle coated with thin film of Pt by e-beam evaporation. [15] c) Elemental gold deposited onto the Pt-nanoseeds by glancing angle deposition (GLAD) producing 30 nm Pt-Au Janus nanomotors. [16]. (b, and c reproduced with permission from [15] and [16], respectively.)

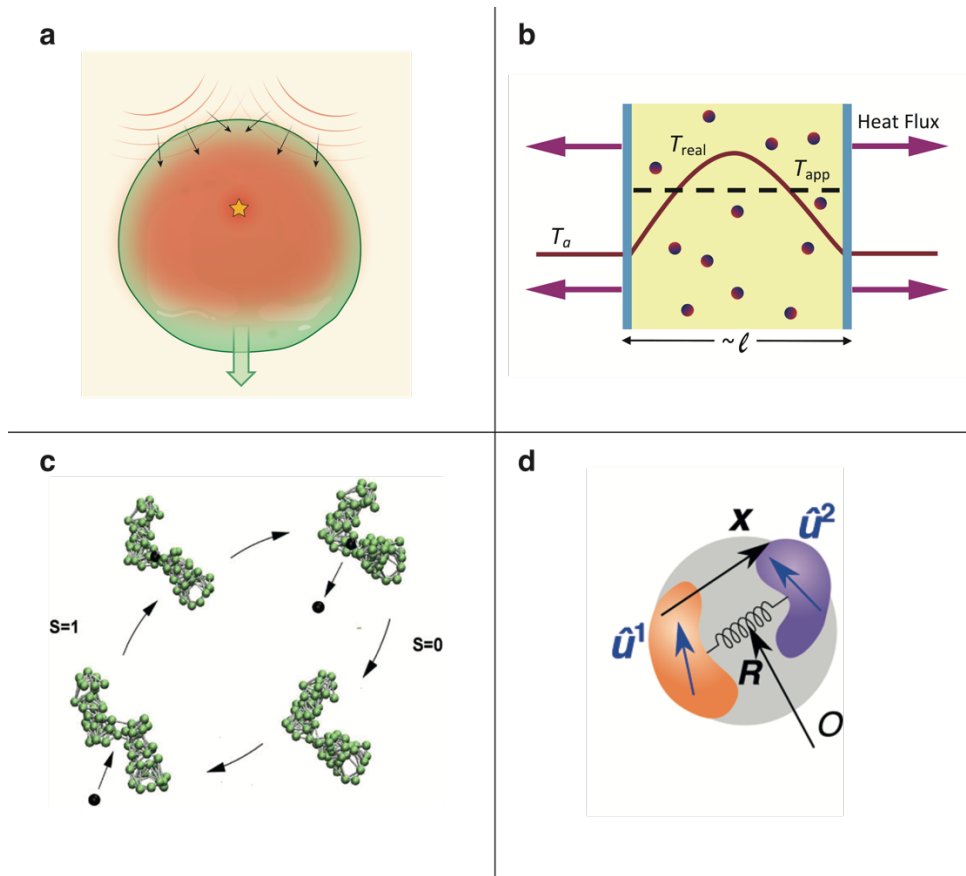


Figure 2 *Enzyme self-propulsion models* a) *Chemoacoustic model*: heat released at the active site (yellow star) by a chemical reaction generates a deformation wave that compresses the enzyme and causes it to move [19]. b) *Collective heating model*: collective heating of the container contributes to the enhanced diffusion of enzymes. The diagram illustrates the heat flux and temperature profile in the chamber containing active enzymes [41]. c) *Stochastic swimming*: the conformational cycle of a model molecular machine is shown. In this non-equilibrium cycle, fast conformation changes are induced by ligand binding and unbinding, which create a force dipole around the enzyme [42,43]. d) *Asymmetric dumbbell model*: two subunits, which represent the modular structure of the enzyme, interact via hydrodynamic interactions and a harmonic-like potential. The enzyme alternates between two equilibrium states: free and bound, which have different mobilities. This model neglects non-equilibrium steps of the reaction and does not depend on exothermicity [21,44]. Reproduced with permission from [19,41,43,44]

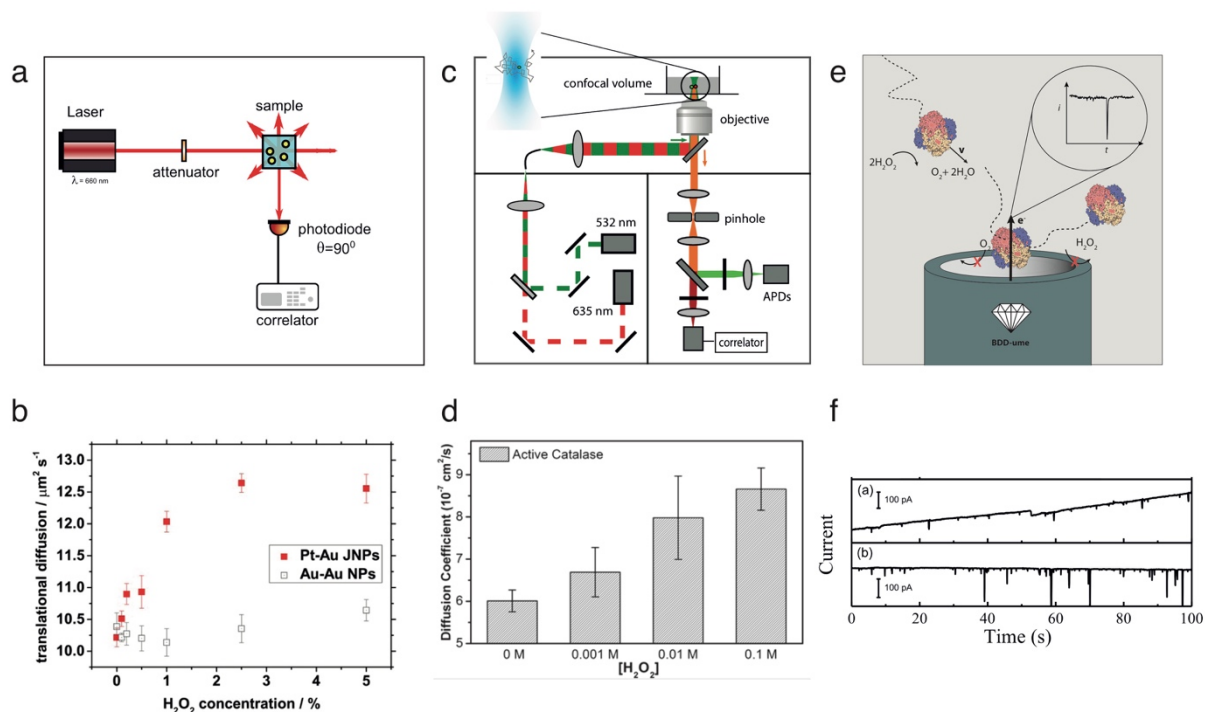


Figure 3 *Experimental methods for self-propulsion measurements.* a) *Dynamic Light Scattering setup.* A laser beam is passed through a polarizer and into a sample. The scattered light is collected by a photomultiplier and a correlator generates the autocorrelation of the intensity trace. b) DLS measurement of translational diffusion constants of 30 nm Pt-Au and Au-Au Janus NPs for different concentrations of H_2O_2 [16]. c) *Fluorescence correlation spectroscopy (FCS) confocal setup.* Lasers are coupled to an objective and a dichroic mirror separates excitation and emission, which is then filtered through the confocal pinhole and detected at avalanche photodiodes. A digital correlator computes the autocorrelation function to extract diffusion constants. d) Diffusion coefficients of catalase at different hydrogen peroxide concentrations measured with FCS [20]. e) *Nanoimpact voltammetry setup* showing collisions of catalase on a boron-doped diamond ultramicroelectrode which translates into current spikes [30]. f) Typical $i-t$ curve at BDD-ume containing (a) 10 pM catalase and (b) 10 pM catalase mixed with 100 mM H_2O_2 . (b,d and f reproduced with permission from [16,20,30], respectively.)

Table 1: List of proposed mechanisms that can lead to enhanced diffusion of catalytically active enzymes.

Mechanism	Description	Reference
<i>Self-electrophoresis</i>	Self-generated gradients of ionic products create flow fields that propel the enzyme.	[18]
<i>Chemoacoustic model</i>	heat released during catalysis generates an asymmetric pressure wave.	[19]
<i>Collective heating</i>	temperature rise caused by the accumulation of reaction heat leads to protein denaturation.	[41]
<i>Stochastic swimming</i>	non-equilibrium cyclic conformational changes create a force dipole.	[42,43]
<i>Asymmetric dumbbell model</i>	The enzyme alternates between two equilibrium states. Its subunits interact via hydrodynamic interactions.	[21,44]

Table 2: Maximum relative increase in diffusion coefficient $(D-D_0)/D_0$ reported for several enzymes. D_0 is the diffusion coefficient in the absence of substrate and ΔH is the reaction enthalpy.

Enzyme	ΔH (kJ mol ⁻¹)	$(D-D_0)/D_0$	References
Catalase	-100	45%	[20]
		30%	[19]
Urease	-59.6	28%	[18]
		25%	[19]
Alkaline Phosphatase	-43.5	80%	[19]
Triose Phosphate Isomerase	-3	not significant	[19]
Aldolase	30-60 (endothermic)	30%	[21]

Table 3:List of experimental methods for measuring self-propulsion of catalytic nanoparticles

Technique	Working principle	Size range	Suitable for	Disadvantages	References
<i>Dynamic Light Scattering (DLS)</i>	Fluctuations in scattered light	<10 μm	Monodisperse colloids	Signal masked by aggregates	[15,16]
<i>Fluorescence Correlation Spectroscopy (FCS)</i>	Fluctuations in fluorescence	<200-300 nm	Fluorescent particles	Needs fluorescence. Limited by confocal volume.	[18,19,20,21]
<i>Optical microscopy</i>	Optical tracking with camera	>200 nm	Large particles	Limited by microscope resolution and camera.	[25]
<i>Nanoparticle Tracking (NTA)</i>	Tracking of scattered light	10-2x10 ³ nm	Nanoparticles	Limited by low scattering of small particles.	[31]
<i>Nanoimpact voltammetry</i>	Particle collisions with electrode	1.5-100 nm (UME) >1 μm (ME)	Metallic NP and proteins	Limited to certain NP and proteins	[30]

References

- [1] M.C. Marchetti, J.F. Joanny, S. Ramaswamy, T.B. Liverpool, J. Prost, M. Rao, R.A. Simha, *Rev. Mod. Phys.* 85 (2013) 1143–1189.
- [2] W.F. Paxton, K.C. Kistler, C.C. Olmeda, A. Sen, S.K. St Angelo, Y.Y. Cao, T.E. Mallouk, P.E. Lammert, V.H. Crespi, *J. Am. Chem. Soc.* 126 (2004) 13424–13431.
- [3] J.R. Howse, R.A. Jones, A.J. Ryan, T. Gough, R. Vafabakhsh, R. Golestanian, *Phys. Rev. Lett.* 99 (2007) 048102.
- [4] P.H. Colberg, S.Y. Reigh, B. Robertson, R. Kapral, *Accounts of Chemical Research* 47 (2014) 3504–3511.
- [5] A.P. Solon, J. Stenhammar, R. Wittkowski, M. Kardar, Y. Kafri, M.E. Cates, J. Tailleur, *Phys. Rev. Lett.* 114 (2015) 198301.
- [6] C. Bechinger, R. Di Leonardo, H. Löwen, C. Reichhardt, G. Volpe, G. Volpe, *Rev. Mod. Phys.* 88 (2016) 045006.
- [7] E.M. Purcell, *Am. J. Phys* 45 (1977) 3–11.
- [8] J.G. Gibbs, Y.P. Zhao, *Applied Physics Letters* 94 (2009).
- [9] G. Ruckner, R. Kapral, *Phys. Rev. Lett.* 98 (2007) 150603.
- [10] J.R. Howse, R.A.L. Jones, A.J. Ryan, T. Gough, R. Vafabakhsh, R. Golestanian, *Phys. Rev. Lett.* 99 (2007) 048102.
- [11] S. Ebbens, M.-H. Tu, J.R. Howse, R. Golestanian, *Phys. Rev. E* 85 (2012) 020401.
- [12] R. Golestanian, T.B. Liverpool, A. Ajdari, *Phys. Rev. Lett.* 94 (2005) 220801.
- [13] J.L. Moran, P.M. Wheat, J.D. Posner, *Phys. Rev. E* 81 (2010) 53.
- [14] R. Kapral, *The Journal of Chemical Physics* 138 (2013) 020901–11.
- [15] X. Ma, K. Hahn, S. Sanchez, *J. Am. Chem. Soc.* 137 (2015) 4976–4979.
- [16] T.-C. Lee, M. Alarcón-Correa, C. Miksch, K. Hahn, J.G. Gibbs, P. Fischer, *Nano Lett.* 14 (2014) 2407–2412.
- [17] R.J. Archer, A.J. Parnell, A.I. Campbell, J.R. Howse, S.J. Ebbens, *Advanced Science* 130 (2017) 1700528.
- [18] H.S. Muddana, S. Sengupta, T.E. Mallouk, A. Sen, P.J. Butler, *J. Am. Chem. Soc.* 132 (2010) 2110–2111.
- [19] C. Riedel, R. Gabizon, C.A. Wilson, K. Hamadani, K. Tsekouras, S. Marqusee, S. Presse, C. Bustamante, *Nature* 517 (2015) 227–230.
- [20] S. Sengupta, K.K. Dey, H.S. Muddana, T. Tabouillot, M.E. Ibele, P.J. Butler, A. Sen, *J. Am. Chem. Soc.* 135 (2013) 1406–1414.
- [21] P. Illien, X. Zhao, K.K. Dey, P.J. Butler, A. Sen, R. Golestanian, *Nano Lett.* 17 (2017) 4415–4420.
- [22] X. Zhao, K.K. Dey, S. Jeganathan, P.J. Butler, U.M. Córdoba-Figueroa, A. Sen, *Nano Lett.* 17 (2017) 4807–4812.
- [23] S. Sengupta, D. Patra, I. Ortiz-Rivera, A. Agrawal, S. Shklyaev, K.K. Dey, U. Córdoba-Figueroa, T.E. Mallouk, A. Sen, *Nature Chemistry* 6 (2014) 415–422.
- [24] X. Bai, P.G. Wolynes, *The Journal of Chemical Physics* 143 (2015) 165101.
- [25] G. Dunderdale, S. Ebbens, P. Fairclough, J. Howse, *Langmuir* 28 (2012) 10997–11006.
- [26] S. Sengupta, M.M. Spiering, K.K. Dey, W. Duan, D. Patra, P.J. Butler, R.D. Astumian, S.J. Benkovic, A. Sen, *ACS Nano* 8 (2014) 2410–2418.
- [27] S.V. Sokolov, S. Eloul, E. Kätelhön, C. Batchelor-McAuley, R.G. Compton, *Physical Chemistry Chemical Physics* 19 (2017) 28–43.
- [28] X. Xiao, A.J. Bard, *J. Am. Chem. Soc.* 129 (2007) 9610–9612.
- [29] J.G.S. Moo, M. Pumera, *ACS Sensors* 6 (2016) 338–345.
- [30] L. Jiang, I. Santiago, J. Foord, *Chem. Commun.* 53 (2017) 8332–8335.
- [31] Y. Tu, F. Peng, X. Sui, Y. Men, P.B. White, J.C.M. van Hest, D.A. Wilson, *Nature Chemistry* 9 (2017) 480–486.
- [32] J. Park, H. Elmlund, P. Ercius, J.M. Yuk, D.T. Limmer, Q. Chen, K. Kim, S.H. Han, D.A. Weitz, A. Zettl, A.P. Alivisatos, *Science* 349 (2015) 290–295.

- [33] R.A. Pavlick, K.K. Dey, A. Sirjoosingh, A. Benesi, A. Sen, *Nanoscale* 5 (2013) 1301–1304.
- [34] C.J. Wienken, P. Baaske, U. Rothbauer, D. Braun, S. Duhr, *Nature Communications* 1 (2010).
- [35] P.H. Colberg, R. Kapral, *EPL (Europhysics Letters)* 106 (2014) 30004.
- [36] P.H. Colberg, R. Kapral, *The Journal of Chemical Physics* 143 (2015) 184906.
- [37] F. Peng, Y. Tu, D.A. Wilson, *Chemical Society Reviews* 46 (2017) 5289–5310.
- [38] J.D. Brodin, E. Auyeung, C.A. Mirkin, *Proc. Natl. Acad. Sci. U.S.a.* 112 (2015) 4564–4569.
- [39] C. Timm, C.M. Niemeyer, *Angewandte Chemie International Edition* 54 (2015) 6745–6750.
- [40] J.B. Trads, T. Tørring, K.V. Gothelf, *Accounts of Chemical Research* 50 (2017) 1367–1374.
- [41] R. Golestanian, *Phys. Rev. Lett.* 115 (2015) 108102.
- [42] A.S. Mikhailov, R. Kapral, *Proc Natl Acad Sci U S A* 112 (2015) E3639–44.
- [43] T. Sakaue, R. Kapral, A.S. Mikhailov, *The European Physical Journal B* 75 (2010) 381–387.
- [44] P. Illien, T. Adeleke-Larodo, R. Golestanian, *EPL (Europhysics Letters)* 119.4 (2017): 40002.